Electronic Supplementary Material (ESI) for Materials Advances.

[Supplementary Information]

Spider Silk-inspired Peptide Multiblock Hybrid Copolymers for Self-healable Thin Film Materials

Tomoyuki Koga[1,] Tomotaka Morishita[1], Yushi Harumoto[1],*

Shin-nosuke Nishimura[2], Nobuyuki Higashi[1]*

[1]Department of Molecular Chemistry and Biochemistry, Faculty of Science and Engineering, Doshisha University, Kyotanabe, Kyoto 610-0321, JAPAN

[2]Institute for Materials Chemistry and Engineering, Kyushu University, Fukuoka 819-0395, JAPAN

Corresponding Author

*E-mail: tkoga@mail.doshisha.ac.jp (T. K.)

*E-mail: nhigashi@mail.doshisha.ac.jp (N. H.)

Synthesis of amine-terminated self-assembling oligopeptides

Amine-terminated oligopeptides with different chain lengths and sequences ($(Ala)_6$, $(Ala)_8$, $(Ala)_{10}$, $(Gly)_8$, $(Leu)_8$, and $(Val)_8$) were synthesized *via* SPPS using 9-fluorenylmethoxycarbonyl (Fmoc) chemistry. The oligo(Ala) blocks were first synthesized on a H_2N-$(CH_2)_2$-NH-Trt-resin using Fmoc-L-Ala-OH, Fmoc-Gly-OH, Fmoc-L-Val-OH, Fmoc-L-Leu-OH, Fmoc-β-Ala-OH, Fmoc-*deg*-COOH (3 equiv), HOBt (3 equiv), and DIPC (3 equiv) in DMF for coupling and piperidine (25%)/DMF for Fmoc removal. Fmoc-*deg*-COOH was introduced at the *C*- and *N*-termini of the peptide as a spacer. To cleave the peptide from the resin, the resin was treated with TFA/TIPS/DCM (10/5/85 [v/v/v]). The resultant amine-terminated oligopeptides were purified *via* a reprecipitation method using diethyl ether and identified *via* ^{1}H NMR and MALDI-TOF MS analyses (Fig. S1).

H_2N-*deg*-$(Ala)_n$-*deg*-NH_2

MALDI-TOFMS: *n*=6; *m/z* 849.1 $[M+H]^+$, 871.1 $[M+Na]^+$ (849.0 $[M+H]^+_{Theory}$, 871.0 $[M+ Na]^+_{Theory}$), *n*=8; *m/z* 991.7 $[M+H]^+$, 1013.5 $[M+Na]^+$ (991.1 $[M+H]^+_{Theory}$, 1013.1 $[M+ Na]^+_{Theory}$), *n*=10; *m/z* 1133.3 $[M+H]^+$, 1155.2 $[M+Na]^+$, 1171.2 $[M+K]^+$ (1133.3 $[M+H]^+_{Theory}$, 1155.3 $[M+ Na]^+_{Theory}$, 1171.4 $[M+ K]^+_{Theory}$). ^{1}H NMR (D_2O, DSS): 1.4 ppm (-CH_3 : side chain of Ala), 2.7 ppm (H_2N-CH_2CH_2-CO-), 3.2-3.3 ppm (-CH_2NH_2), 3.4-3.5 ppm (-NH-CH_2CH_2-O-), 3.6 ppm (-NHCH_2CH_2NH-), 3.65 ppm (-NHCH_2CH_2O-), 3.75 ppm (-OCH_2CH_2O-), 4.1-4.4 ppm (α-C*H* : main chain of Ala, -OCH_2CO-).

H_2N-*deg*-$(Gly)_8$-*deg*-NH_2

MALDI-TOFMS: *m/z* 878.1 $[M+H]^+$, 900.1 $[M+Na]^+$ (877.9 $[M+H]^+_{Theory}$, 899.9 $[M+ Na]^+_{Theory}$). ^{1}H NMR (D_2O, DSS): 2.7 ppm (H_2N-CH_2CH_2-CO-), 3.2-3.3 ppm (-CH_2NH_2), 3.4-3.5 ppm (-NH-CH_2CH_2-O-), 3.6 ppm (-NH$CH_2CH_2NH_2$), 3.65 ppm (-NHCH_2CH_2O-), 3.7-3.8 ppm (-OCH_2CH_2O-), 4.0-4.3 ppm (-CH_2- : main chain of Gly, -OCH_2CO-).

H_2N-*deg*-$(Val)_8$-*deg*-NH_2

MALDI-TOFMS: *m/z* 1237.9 $[M+Na]^+$, 1253.9 $[M+K]^+$ (1237.8 $[M+ Na]^+_{Theory}$, 1253.9 $[M+ K]^+_{Theory}$). ^{1}H NMR (D_2O/TFA, DSS): 1.0-1.2 ppm (-CH$(CH_3)_2$: side chain of Val), 2.2 ppm (-C*H*$(CH_3)_2$: side chain of Val), 2.9 ppm (H_2N-CH_2CH_2-CO-), 3.4-3.6 ppm (-CH_2NH_2, -NH-CH_2CH_2-O-), 3.7-3.8 ppm (-NH$CH_2CH_2NH_2$, -NHCH_2CH_2O-), 3.9 ppm (-OCH_2CH_2O-), 4.2-4.6 ppm (α-C*H* : main chain of Val, -OCH_2CO-).

H_2N-*deg*-$(Leu)_8$-*deg*-NH_2

MALDI-TOFMS: *m/z* 1350.5 $[M+Na]^+$, 1365.6 $[M+K]^+$ (1349.5 $[M+ Na]^+_{Theory}$, 1365.6 $[M+ K]^+_{Theory}$). ^{1}H NMR (D_2O/TFA, DSS): 0.9-1.1 ppm (-CH$(CH_3)_2$:side chain of Leu), 1.6-2.0 ppm (-CH_2CH$(CH_3)_2$, -CH_2C*H*$(CH_3)_2$: side chain of Leu), 2.8 ppm (H_2N-CH_2CH_2-CO-), 3.3-3.5 ppm (-CH_2NH_2), 3.5-3.7 ppm (-NH-CH_2CH_2-O-, -NH$CH_2CH_2NH_2$), 3.7-3.8 ppm (-NHCH_2CH_2O-), 3.8 ppm (-OCH_2CH_2O-), 4.1-4.4 ppm (α-C*H* : main chain of Leu, -OCH_2CO-).

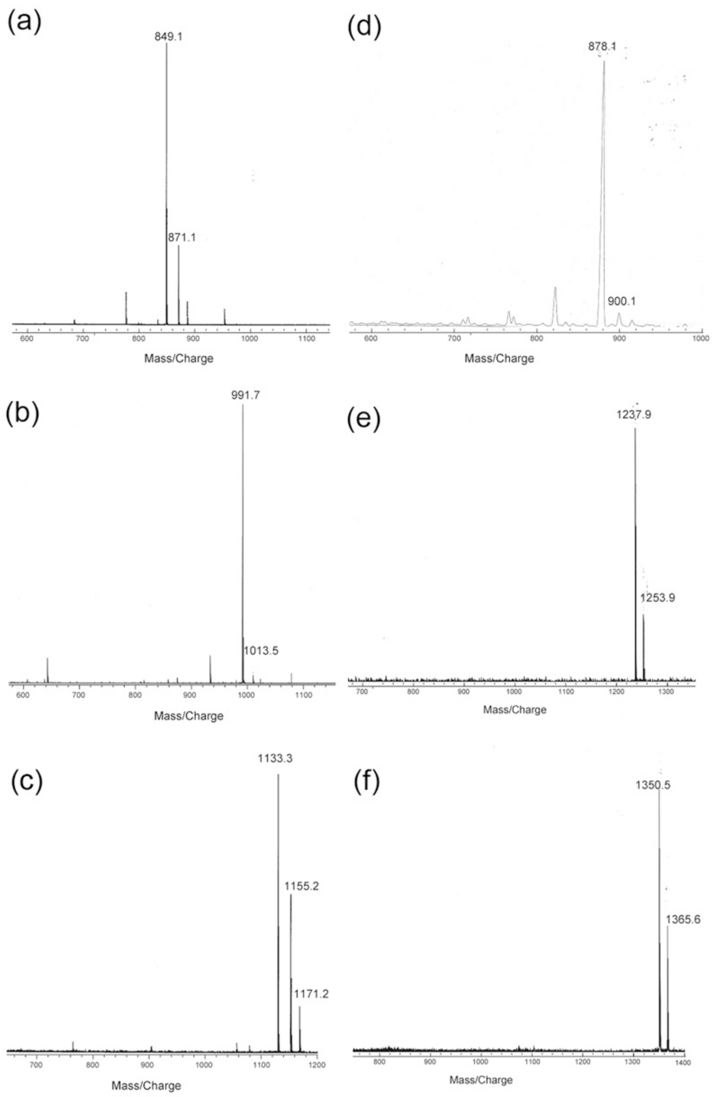

Figure S1. MALDI TOF MS spectra of H_2N-*deg*-(Ala)$_6$-*deg*-NH_2 (a), H_2N-*deg*-(Ala)$_8$-*deg*-NH_2 (b), H_2N-*deg*-(Ala)$_{10}$-*deg*-NH_2 (c), H_2N-*deg*-(Gly)$_8$-*deg*-NH_2 (d), H_2N-*deg*-(Val)$_8$-*deg*-NH_2 (e), and H_2N-*deg*-(Leu)$_8$-*deg*-NH_2 (f). Matrix: CHCA.

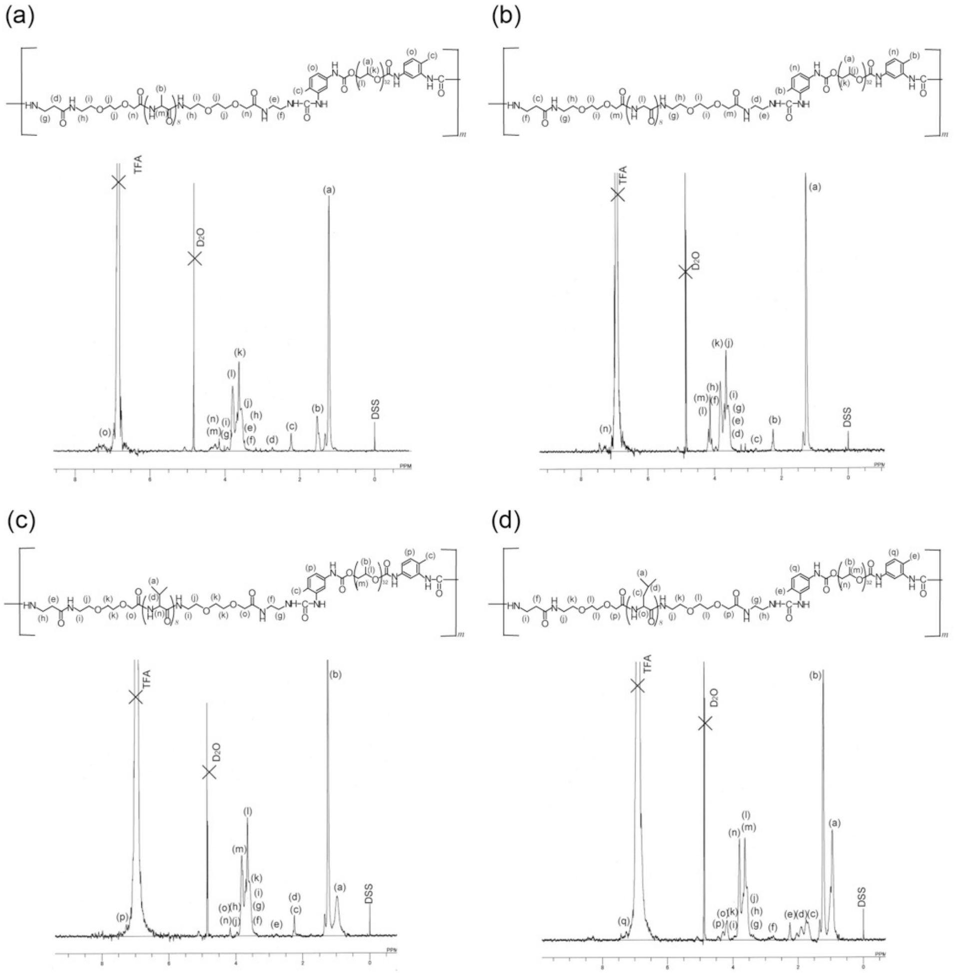

Figure S2. ^{1}H-NMR spectra of $[(Ala)_8\text{-PPG}]_m$ (a), $[(Gly)_8\text{-PPG}]_m$ (b), $[(Val)_8\text{-PPG}]_m$ (c), and $[(Leu)_8\text{-PPG}]_m$ (d) in D_2O containing TFA at 20 °C.

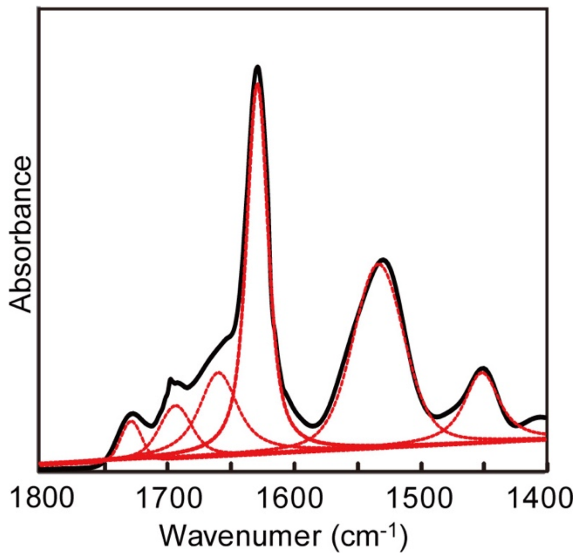

Figure S3. Peak deconvolution of FTIR spectrum of [(Ala)$_{10}$-PPG]$_m$ microfilm (~40 μm thick).

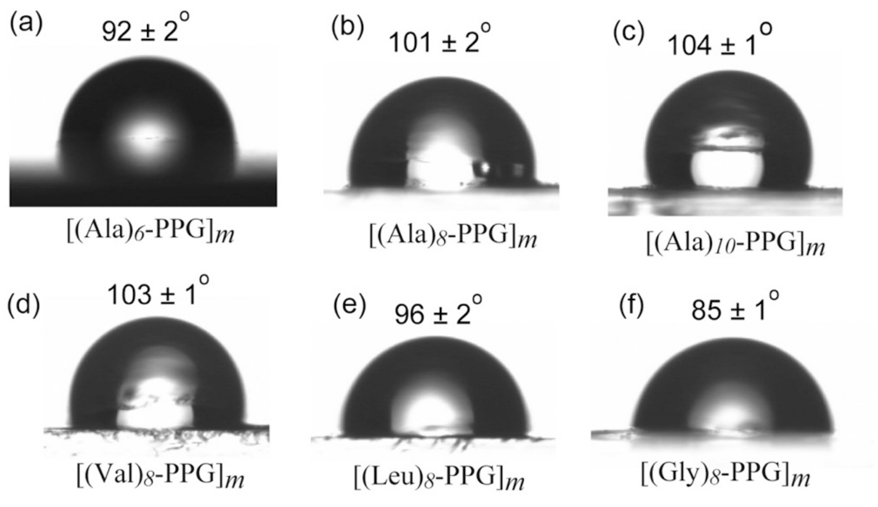

Figure S4. Water contact angles for various multiblock polymer films. (a) [(Ala)$_6$-PPG]$_m$, (b) [(Ala)$_8$-PPG]$_m$, (c) [(Ala)$_{10}$-PPG]$_m$, (d) [(Val)$_8$-PPG]$_m$, (e) [(Leu)$_8$-PPG]$_m$, and (f) [(Gly)$_8$-PPG]$_m$ films.

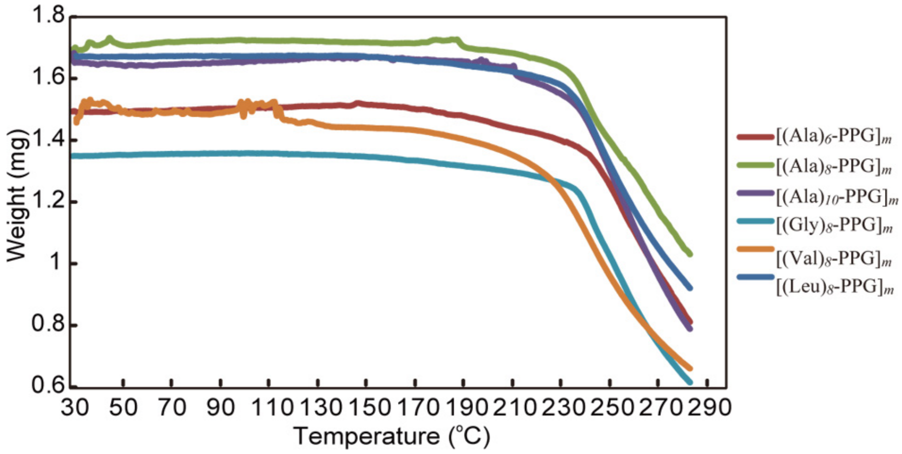

Figure S5. Thermogravimetric analyses of various $[(\text{peptide})_n\text{-PPG}]_m$ films.

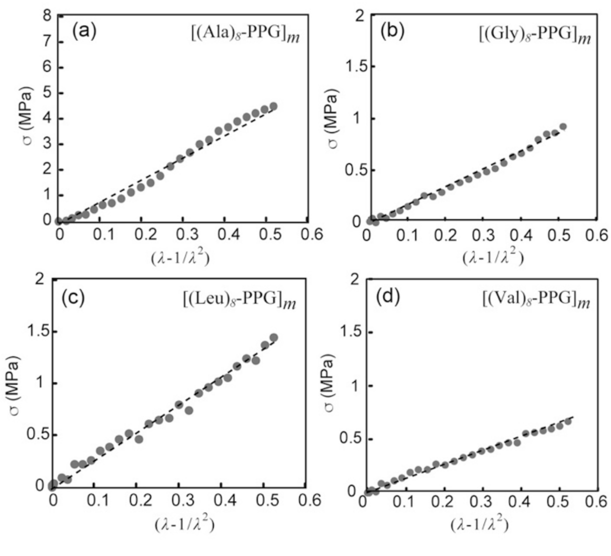

Figure S6. Stress vs. (λ-1/λ^2) for various $[(\text{peptide})_8\text{-PPG}]_m$ microfilms, where slopes indicate shear modulus *G*.

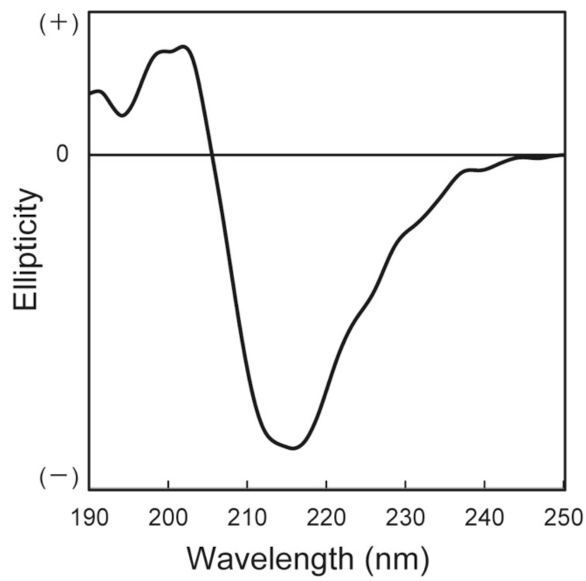

Figure S7. CD spectrum of [(Ala)$_{10}$-PPG]$_m$ nanofilm (300 nm thickness) on quartz plate.

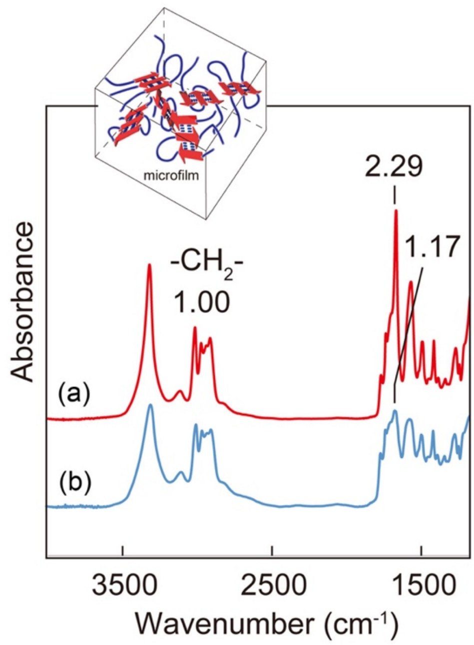

Figure S8. (a) Transmission– and (b) reflection absorption–FTIR spectra of [(Ala)$_{10}$-PPG]$_m$ microfilm (~40 μm thick) on CaF_2 and Au plates, respectively.

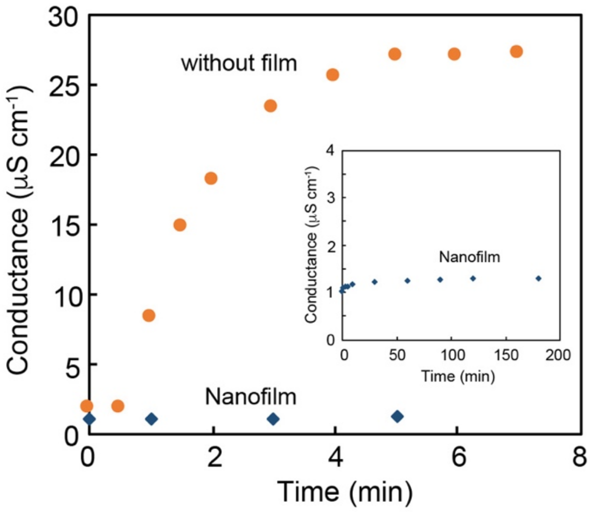

Figure S9. Time courses of ion permeation (*p*TSNa) through [(Ala)$_{10}$-PPG]$_m$ nanofilm (300 nm thick). Inset shows time course of electrical conductance over a long duration (180 min).

Table S1. Film thickness of [(Ala)$_n$-PPG]$_m$-nanofilms estimated *via* AFM and SEM analyses.

		Polymer Concentration		
Polymer		0.5 wt%	1.0 wt%	2.0 wt%
[(Ala)$_6$-PPG]$_m$	AFM	50 nm	100 nm	290 nm
	SEM	60 nm	110 nm	300 nm
[(Ala)$_8$-PPG]$_m$	AFM	50 nm	170 nm	300 nm
	SEM	70 nm	150 nm	300 nm
[(Ala)$_{10}$-PPG]$_m$	AFM	140 nm	180 nm	290 nm
	SEM	150 nm	200 nm	300 nm